

# Synaptic Properties of Thalamic Input to Layers 2/3 and 4 of Primary Somatosensory and Auditory Cortices

Angela N. Viaene, Iraklis Petrof and S. Murray Sherman

*J Neurophysiol* 105:279-292, 2011. First published 3 November 2010; doi:10.1152/jn.00747.2010

**You might find this additional info useful...**

---

Supplemental material for this article can be found at:

<http://jn.physiology.org/content/suppl/2010/11/19/jn.00747.2010.DC1.html>

This article cites 49 articles, 25 of which can be accessed free at:

<http://jn.physiology.org/content/105/1/279.full.html#ref-list-1>

Updated information and services including high resolution figures, can be found at:

<http://jn.physiology.org/content/105/1/279.full.html>

Additional material and information about *Journal of Neurophysiology* can be found at:

<http://www.the-aps.org/publications/jn>

---

This information is current as of February 3, 2011.

# Synaptic Properties of Thalamic Input to Layers 2/3 and 4 of Primary Somatosensory and Auditory Cortices

Angela N. Viaene,\* Iraklis Petrof,\* and S. Murray Sherman

Department of Neurobiology, University of Chicago, Chicago, Illinois

Submitted 30 August 2010; accepted in final form 28 October 2010

**Viaene AN, Petrof I, Sherman SM.** Synaptic properties of thalamic input to layers 2/3 and 4 of primary somatosensory and auditory cortices. *J Neurophysiol* 105: 279–292, 2011. First published November 3, 2010; doi:10.1152/jn.00747.2010. We studied the synaptic profile of thalamic inputs to cells in layers 2/3 and 4 of primary somatosensory (S1) and auditory (A1) cortices using thalamocortical slices from mice age postnatal days 10–18. Stimulation of the ventral posterior medial nucleus (VPM) or ventral division of the medial geniculate body (MGBv) resulted in two distinct classes of responses. The response of all layer 4 cells and a minority of layers 2/3 cells to thalamic stimulation was Class 1, including paired-pulse depression, all-or-none responses, and the absence of a metabotropic component. On the other hand, the majority of neurons in layers 2/3 showed a markedly different, Class 2 response to thalamic stimulation: paired-pulse facilitation, graded responses, and a metabotropic component. The Class 1 and Class 2 response characteristics have been previously seen in inputs to thalamus and have been described as drivers and modulators, respectively. Driver input constitutes a main information bearing pathway and determines the receptive field properties of the postsynaptic neuron, whereas modulator input influences the response properties of the postsynaptic neuron but is not a primary information bearing input. Because these thalamocortical projections have comparable properties to the drivers and modulators in thalamus, we suggest that a driver/modulator distinction may also apply to thalamocortical projections. In addition, our data suggest that thalamus is likely to be more than just a simple relay of information and may be directly modulating cortex.

## INTRODUCTION

A proper classification of constituent elements has always been a key early step in understanding the brain; a clear example is the classification of different neuronal types in many regions, including retina and cortex. This approach applies as well to afferent input classes as an important variable constituent of complex circuits. That is, just as one must appreciate the different neuronal classes to understand retina or cortex, we argue that one must have a proper classification of synaptic inputs to understand circuits, and this is especially important for glutamatergic inputs, which dominate in the brain.

Such a classification has proven to be useful in parsing thalamic circuitry, for which two distinct types of glutamatergic input have been described (Sherman and Guillery 1998) and termed *drivers* and *modulators*. Examples of the former are retinal (or medial lemniscal) input to the lateral geniculate nucleus (or ventral posterior medial nucleus), and these pro-

vide the main information to be relayed; examples of the latter are the layer 6 feedback projections to thalamic relay cells, and these are organized to modulate transmission of driver input (Li et al. 2003; Petrof and Sherman 2009; Reichova and Sherman 2004).

Our goal in this study is to extend the classification of thalamic inputs to cortex. Prior classification studies described all inputs to layer 4 as drivers (Lee and Sherman 2008), whereas studies focusing on other cortical layers have not made a detailed attempt to classify the thalamocortical inputs (Tan et al. 2008; Zhou et al. 2010). We extend this by using the thalamocortical slice preparation in the mouse somatosensory and auditory systems to describe the properties of thalamocortical input to layers 2/3. We found that, although all thalamocortical inputs to layer 4 indeed have properties similar to those of drivers in thalamus, only some to layers 2/3 have these properties, and the majority of responsive neurons have properties similar to those of modulators in thalamus. An abstract of this has been submitted to the Society for Neuroscience for the 2010 meeting.

## METHODS

### *Slice preparation*

All procedures described below were in accordance with guidelines of the Institutional Animal Care and Use Committee at the University of Chicago. BALB/c mice (age 10–18 days) were anesthetized with a few drops of isoflurane placed in a cotton wool within a transparent chamber and decapitated. Brains were quickly removed and placed in chilled (0–4°C), oxygenated (95% O<sub>2</sub>-5% CO<sub>2</sub>) slicing solution containing the following (in mM): 2.5 KCl, 1.25 NaH<sub>2</sub>PO<sub>4</sub>, 10 MgCl<sub>2</sub>, 0.5 CaCl<sub>2</sub>, 26 NaHCO<sub>3</sub>, 11 glucose, and 206 sucrose. Five hundred-micrometer-thick thalamocortical slices were prepared as previously reported (Cruikshank et al. 2002; Llinas et al. 2002), and this is briefly described here. For the somatosensory cortex experiments, the brain was blocked at a 45–50° angle from the midsagittal plane, and the blocked side was glued onto a vibratome platform (Leica, Wetzlar, Germany) for sectioning. For the auditory cortex experiments, the brain was blocked at a 25° angle rostrocaudally from the dorsal surface, and the blocked surface was placed facing down. A 15° off-horizontal cut was made along the mediolateral plane, and this blocked surface was glued onto the vibratome platform for sectioning.

Once cut, slices from either preparation were placed in warm (32°C) oxygenated artificial cerebrospinal fluid (ACSF) containing (in mM) 125 NaCl, 3 KCl, 1.25 NaH<sub>2</sub>PO<sub>4</sub>, 1 MgCl<sub>2</sub>, 2 CaCl<sub>2</sub>, 25 NaHCO<sub>3</sub>, and 25 glucose and were allowed to recover for at least an additional 30 min at room temperature before being used. Once in the recording chamber, slices were continuously perfused with oxygenated ACSF at room temperature.

\* A. N. Viaene and I. Petrof contributed equally to this work.

Address for reprint requests and other correspondence: S. M. Sherman, Dept. of Neurobiology, University of Chicago, Abbott J-117, 947 E. 58th St., Chicago, IL 60637 (E-mail: msherman@bsd.uchicago.edu).

### Flavoprotein autofluorescence imaging

At the beginning of an experiment, the connectivity of the two slice preparations was confirmed using flavoprotein autofluorescence (FA) imaging (Llano et al. 2009). FA captures green light (520–560 nm) emitted by mitochondrial flavoproteins exposed to blue light (472–488 nm) in conditions of metabolic activity associated with postsynaptic activation (Llano et al. 2009; Shibuki et al. 2003). Once a particular area of tissue has been stimulated, FA uses the elevated levels of mitochondrial green light emissions to detect cellular activation in remote areas of the tissue, a sign of connectivity. FA was carried out using a QImage Retiga-SRV camera (QImaging, Surrey, BC, Canada) attached onto a fluorescence microscope (Axioscop 2FS, Carl Zeiss Instruments, Jena, Germany). For any given trial, FA activity was recorded over the whole slice for a total of 14 s, including 1.5 s before stimulation [10 pulses at 20 Hz and 150–300  $\mu$ A, over the ventral posterior medial nucleus (VPM) or the ventral division of the medial geniculate body (MGBv)] and 12 s after stimulation. FA images were acquired at 2.5–10 frames per second (integration time of 100–400 ms). The final image was generated as a function of the  $\Delta f/f$  ratio of the baseline autofluorescence of the slice before stimulation subtracted from the autofluorescence of the slice over the period of stimulation ( $\Delta f$ ) divided by baseline ( $f$ ). Individual cortical layers in FA images were identified by overlaying brightfield images of the slices.

### Electrophysiology

Current-clamp and voltage-clamp mode whole cell recordings were carried out in a visualized slice setup under a DIC-equipped microscope and with a Multiclamp 700B amplifier and pCLAMP software (Axon Instruments, Union City, CA). Recording glass pipettes with input resistances ranging between 3 and 7 M $\Omega$ , were filled with intracellular solution containing (in mM) 117 K-gluconate, 13 KCl, 1 MgCl<sub>2</sub>, 0.07 CaCl<sub>2</sub>, 10 HEPES, 0.1 EGTA, 2 Na<sub>2</sub>-ATP, 0.4 Na-GTP, 0.003 TS-TM calix[4]arene, and 0.02% biocytin; pH 7.3, 290 mOsm. We included TS-TM calix[4]arene (0.003 mM), a chloride channel blocker, to our intracellular solution (generously provided by Professor R. J. Bridges of Rosalind Franklin University) to block GABAergic effects on the recorded cell (Dudek and Friedlander 1996). Individual cortical layers (layers 2/3 vs. layer 4) were identified by the marked differences in their brightness under DIC. Transition zones between layers were avoided to minimize the risk of false sampling. Electric stimulation of the thalamocortical pathways was delivered through a concentric bipolar electrode (FHC, Bowdoinham, ME), which carries the advantage of delivering current to a relatively restricted tissue area. Short-term plasticity (paired-pulse depression vs. paired-pulse facilitation) was examined using a stimulation protocol consisting of four 0.3-ms-long positive current pulses at a frequency of 10 Hz. To minimize further the spread of the passed current (which could potentially result in the recruitment of additional afferent pathways of the recorded area), the assessment of paired-pulse effects was carried out for the lowest stimulation intensity capable of inducing excitatory postsynaptic potentials (EPSPs) of a >0.5 mV amplitude (for  $\geq 3$  of the 4 EPSPs) in the recorded cells, although other experiments were aimed at determining the effects of increased stimulation currents on evoked responses (see RESULTS). For example, we assessed the relationship between the intensity of the stimulation current and the amplitude of the evoked EPSPs by starting at 25  $\mu$ A (which typically was within 10–20  $\mu$ A of the threshold for evoking a synaptic response in each cell) and increasing the stimulation intensity in increments of 25 or 50  $\mu$ A. A high-frequency stimulation (HFS) protocol (0.1-ms-long pulses delivered at 125 Hz over 200–800 ms, 100–300  $\mu$ A) was used for the examination of metabotropic glutamate receptor activation (McCormick and von Krosigk 1992).

NMDA and AMPA receptor antagonists (AP5, 100  $\mu$ M and DNQX, 50  $\mu$ M, respectively) were applied during HFS to isolate any

metabotropic responses. Where long-lasting (>2 s) membrane potential changes were seen under these conditions, the type 1 metabotropic glutamate receptor antagonist LY367385 (40  $\mu$ M) and the type 5 metabotropic glutamate receptor antagonist MPEP (30  $\mu$ M) were used to block them, confirming that they were metabotropic (collectively, type 1 and type 5 metabotropic glutamate receptors are known as group I and will be referred to as such from now on). All data were digitized on a Digidata 1200 board (Axon Instruments) and stored on a computer for off-line analysis. Measurement and analyses of the acquired traces were performed in ClampFit (Axon Instruments) software. Latency was defined as the time between stimulation offset and the beginning of the evoked EPSP. E2/E1 ratio was calculated by dividing the amplitude of the second EPSP by the amplitude of the first EPSP. An E2/E1 ratio >1 indicates paired-pulse facilitation, whereas an E2/E1 ratio <1 indicates paired-pulse depression. The laminar position of connected, layers 2/3 neurons was measured using brightfield images taken during the recording sessions and taken as the radial distance from the boundary between layers 3 and 4.

### Glutamate photo-uncaging

For the photo-uncaging of caged glutamate, nitroindolonyl-caged glutamate (Sigma-Aldrich, St. Louis, MO) was added to the recirculating ACSF (0.4 mM), and a UV laser beam (DPSS Laser, Santa Clara, CA) was used to locally photolyse the caged compound over an 8  $\times$  8 grid in a pseudorandom order that minimized the possibility of sequentially stimulating adjacent spots or locally depleting caged glutamate (Lam and Sherman 2005, 2007; Lam et al. 2006; Shepherd et al. 2003). The laser beam had an intensity of 20–80 mW, and laser illumination lasted 2 ms (355 nm wavelength, frequency-tripled Nd:YVO4, 100 kHz pulse repetition rate). Custom-made software written in Matlab (Mathworks, Natick, MA) was used to control the uncaging interface.

### Neuroanatomical techniques

Animals were anesthetized with a ketamine (100 mg/kg)-xylazine (3 mg/kg) cocktail and placed in a stereotaxic apparatus (Kopf, Tujunga, CA). Responses to tail and toe pinch were monitored, and maintenance doses of anesthesia were administered as required. Stereotaxic coordinates were determined using the Paxinos and Franklin (2008) mouse brain atlas for tracer injections into thalamus (all distances are from Bregma): VPM injections (AP: –1.7, ML:  $\pm$ 1.55, DV: –3.4); MGBv injections (AP: –3.1, ML:  $\pm$ 2.0, DV: –3.35). Bilateral injections of 5% biotinylated dextran amine (BDA 10,000 M.W., Molecular Probes, Eugene, OR) in PBS were done through iontophoresis, using currents of 5–12  $\mu$ A, at 7-s-long ON-OFF cycles, for 15–20 min. Immediately after surgery, animals were treated locally with Lidocaine Hydrochloride jelly (Akorn, Buffalo Grove, IL) and Vetropolycin antibiotic ointment (Dechra VP, Overland Park, KS). In addition, animals received analgesic doses (0.1 mg/kg) of Buprenex (Reckitt Benckiser Healthcare, Hull, UK) every 12 h. After a 72-h postinjection period, the animals were deeply anesthetized with ketamine/xylazine and transcardially perfused with PBS followed by 4% paraformaldehyde in PBS. Brains were subsequently placed in an ascending sucrose gradient (10–30%) until saturated. Fifty-micrometer-thick sections were cut using a sliding microtome. Alternating slices were processed for BDA and Nissl. The following protocol was used for BDA processing. Slices were treated with a 15-min-long wash in 0.5% H<sub>2</sub>O<sub>2</sub>, three washes in PBS, a 0.3% Triton-X wash, and were finally incubated overnight with ABC reagent (Vectastain ABC-Peroxidase Kit, Vector, Burlingame, CA). Subsequently, after two washes in PBS and two washes in Tris-buffered saline, sections were bathed in diaminobenzidine (DAB, SigmaFast, Sigma-Aldrich) to visualize the label. Finally sections were mounted onto gelatinized slides, dehydrated, and cover slipped. This same protocol was used to

process slices from electrophysiology experiments to recover biocytin-filled cells.

Brain sections were examined under a microscope (Leica Microsystems GmbH, Wetzlar, Germany), and photos of terminal fields in layers 2/3 and 4 were taken at 100 $\times$  using a Retiga 2000 monochrome CCD camera and Q Capture Pro software (QImaging). The resolution of the digital images used for the bouton area measurements was 1,600  $\times$  1,200 pixels, and the size of each pixel was 0.075  $\mu$ m. The plane of focus was determined by the researcher taking the photos.

After a photo was taken and code-named to avoid bias, identified patterns of axons and/or boutons at the edges of the photo were used as landmarks for transitioning to directly adjacent areas within the region of interest before the next photo was taken, ensuring that boutons did not appear in multiple photos. AxioVision software (Carl Zeiss Instruments) was used to analyze the coded images and measure the sizes of boutons. Labeled boutons were identified by their round shape and were marked by manually outlining their perimeter, which also prevented repetitive counting. We only performed measurements when there was a clear border between the bouton and the background (i.e., when boutons were in the plane of focus). Boutons that had a shadow around them or that lacked a sharp border were excluded from our measurements to avoid underestimating their true size (i.e., that the largest part of the bouton was outside the plane of focus). Outlines were drawn along the border of the dark bouton and lighter background. Given the limits of the resolution at the light microscopic level with our combination of magnification and numerical aperture have been estimated to be around 0.3  $\mu$ m (Friedlander et al. 1981; Llano and Sherman

2008; Slayter 1970). We excluded any bouton with a diameter of <0.4  $\mu$ m from our measurements. We focused our measurements on layers 2/3 of S1 and A1, layer 4 in A1, and the barrels of layer 4 in S1. One thousand boutons were measured in layers 2/3 and in layer 4 of each cortical area. Nissl-stained sections were used to aid in the identification of boundaries between cortical layers.

RESULTS

FA and glutamate photo-uncaging

Electrical stimulation of VPM in the somatosensory thalamocortical slice resulted in fluorescent activity in S1 as imaged by FA, particularly over layers 4 and 2/3 (Fig. 1A). Similarly, electrical stimulation of MGBv in the auditory thalamocortical slice produced FA activation over middle and upper layers of A1, in addition to activation of the thalamic reticular nucleus (TRN) and patches of basal ganglia (BG) (Fig. 1B).

Because electrical stimulation carries the disadvantage of potentially activating not only cell bodies but also axons (either antidromically or fibers of passage), we wanted to specifically show that input from the thalamic nuclei of interest (VPM and MGBv) could activate cortex. For that purpose, we recorded from cells in layers 2/3 of S1 and A1 in voltage clamp and photostimulated VPM and MGBv, respectively, while bathing

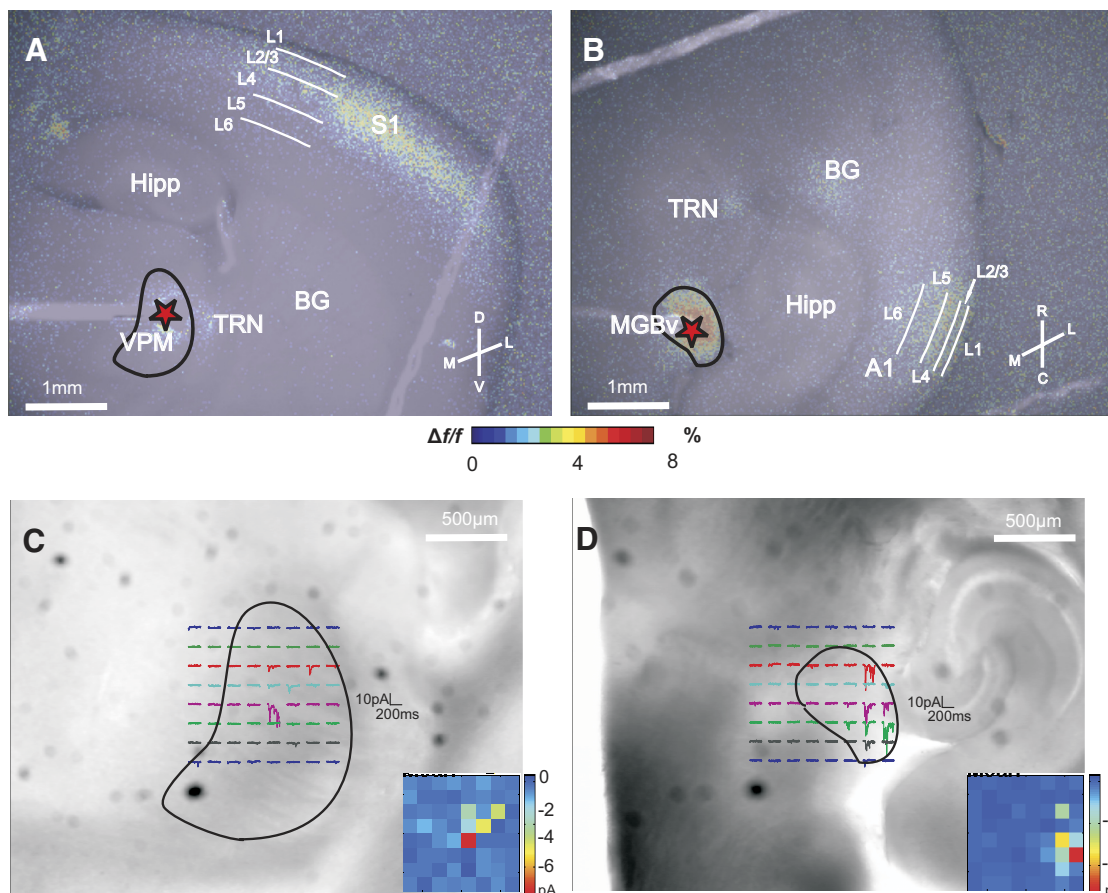


FIG. 1. Slice connectivity verified using flavoprotein autofluorescence (FA) imaging and photo-uncaging of glutamate. Two typical examples where 20 Hz electrical stimulation (150  $\mu$ A) of ventral posterior medial nucleus (VPM) and ventral division of the medial geniculate body (MGBv) (red asterisks) resulted in FA activation in layer 4 and layers 2/3 of S1 (A) and A1 (B), respectively. Color scale represents the % $\Delta f/f$  change in fluorescence. Examples of inward currents recorded from layers 2/3 cells located in S1 (C) and A1 (D) while photo-uncaging glutamate over VPM and MGBv, respectively. Insets: false-color maps of location and magnitude of inward currents. Each pixel corresponds to a locus of uncaging as seen in the main figure. M, medial; L, lateral; D, dorsal; V, ventral; R, rostral; C, caudal; Hipp, hippocampus; TRN, thalamic reticular nucleus; BG, basal ganglia; L1, layer 1; L2/3, layers 2/3; L4, layer 4; L5, layer 5; L6, layer 6.

the slice in caged glutamate. With regard to the somatosensory preparation, inward currents in layers 2/3 of S1 were typically seen after stimulation in the dorsolateral area of VPM (Fig. 1C). Inward currents were also recorded from cells in layers 2/3 of A1 after stimulation of the lateral aspect of MGBv (Fig. 1D). To minimize activating inappropriate axons, we located the electrical stimulating electrodes in thalamus at the site for which photostimulation evoked the largest response, and this site was always located near the center of the region from which responses to photostimulation could be evoked. All subsequent experiments used electrical stimulation.

#### Thalamocortical response classes

**LAYERS 2/3.** We recorded from a total of 127 cells in layers 2/3 of S1, 50 of which responded to extracellular electrical stimulation in the thalamus with EPSPs. We also recorded from a total of 65 cells in layers 2/3 of A1, 26 of which responded to thalamic stimulation with EPSPs. Only the subset of connected cells are considered further. Layers 2/3 cells of S1 had a membrane potential of  $-58.65 \pm 7.45$  (SD) mV, uncorrected for a roughly  $-10$  mV junction potential, and an input resistance of  $418.99 \pm 77.63$  M $\Omega$ . Layers 2/3 cells in A1 had an uncorrected membrane potential of  $-59.75 \pm 6.73$  mV and an input resistance of  $446.48 \pm 78.22$  M $\Omega$ .

We conclude that all of the recorded cells in layers 2/3 in both areas were pyramidal cells for the following reasons (Fig. 2). We visually identified pyramidal cells during recording on the basis of their size and shape and by their response to negative

current injections (presence of  $I_H$ ) and positive current injections (spike frequency adaptation). In addition, all recovered biocytin-filled cells in layers 2/3 ( $n = 38$ ) were pyramidal. In the recovered layers 2/3 neurons, we did not observe any dendrites extending into layer 4.

We found in analyzing the responses to trains of electrical stimulation that two quite different response patterns emerged to thalamocortical stimulation for these layers 2/3 cells, which we term *Class 1* and *Class 2*. The majority of these cells (36 of the 50 in S1 and 20 of the 26 in A1) responded with EPSPs showing the Class 2 pattern. The evoked EPSP started small in amplitude but showed paired-pulse facilitation, meaning that the amplitude of the second evoked EPSP in the series exceeded that of the first (Figs. 3Ai and 4Ai). They also showed a monotonic relationship of increasing EPSP amplitude with increasing stimulation intensity (Figs. 3Ai and 4Ai). The EPSPs evoked at 10 Hz could be blocked by the ionotropic glutamate receptor antagonists DNQX and AP5 (Figs. 3Aii and 4Aii), but higher frequency stimulation (125 Hz for 200–800 ms) evoked prolonged ( $>2$  s) membrane depolarizations that could be blocked with the group I metabotropic glutamate receptor antagonists LY367385 and MPEP (Figs. 3Aiii and 4Aiii).

To determine whether the metabotropic glutamate receptor activation was plausibly postsynaptic, for a subset of the cells in layers 2/3 showing Class 2 responses to thalamic stimulation (5 cells in S1 and 4 in A1), we performed the following additional experiment before applying group I metabotropic glutamate receptor antagonists. We applied the group I

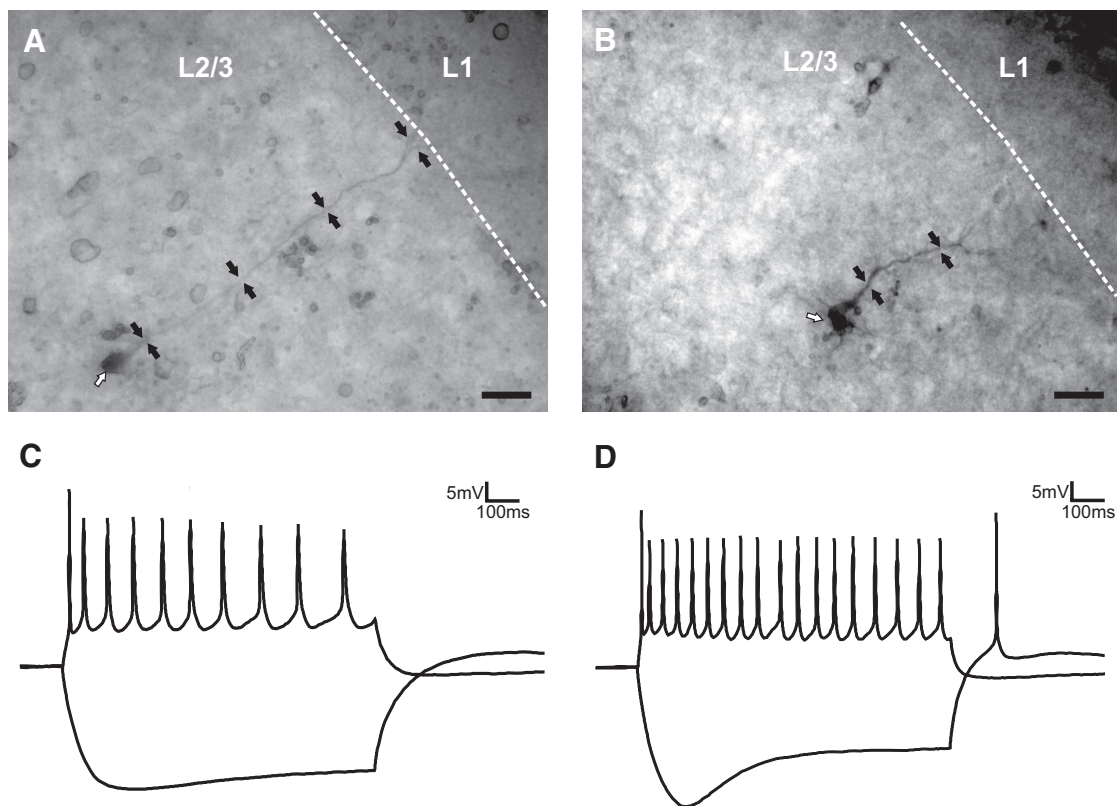


FIG. 2. Morphology and intrinsic properties of pyramidal neurons in layers 2/3. *A*: a biocytin-filled cell in layers 2/3 of S1. *B*: a biocytin-filled cell in layers 2/3 of A1. *C*: responses to positive (100 pA) and negative ( $-100$  pA) current injection of a layers 2/3 pyramidal cell in S1. *D*: responses to positive (100 pA) and negative ( $-100$  pA) current injection of a layers 2/3 pyramidal cell in A1. White arrows in *A* and *B* point to the cell bodies while black arrows highlight the location of the apical dendrites. Scale bars in *A* and *B*: 0.025 mm.

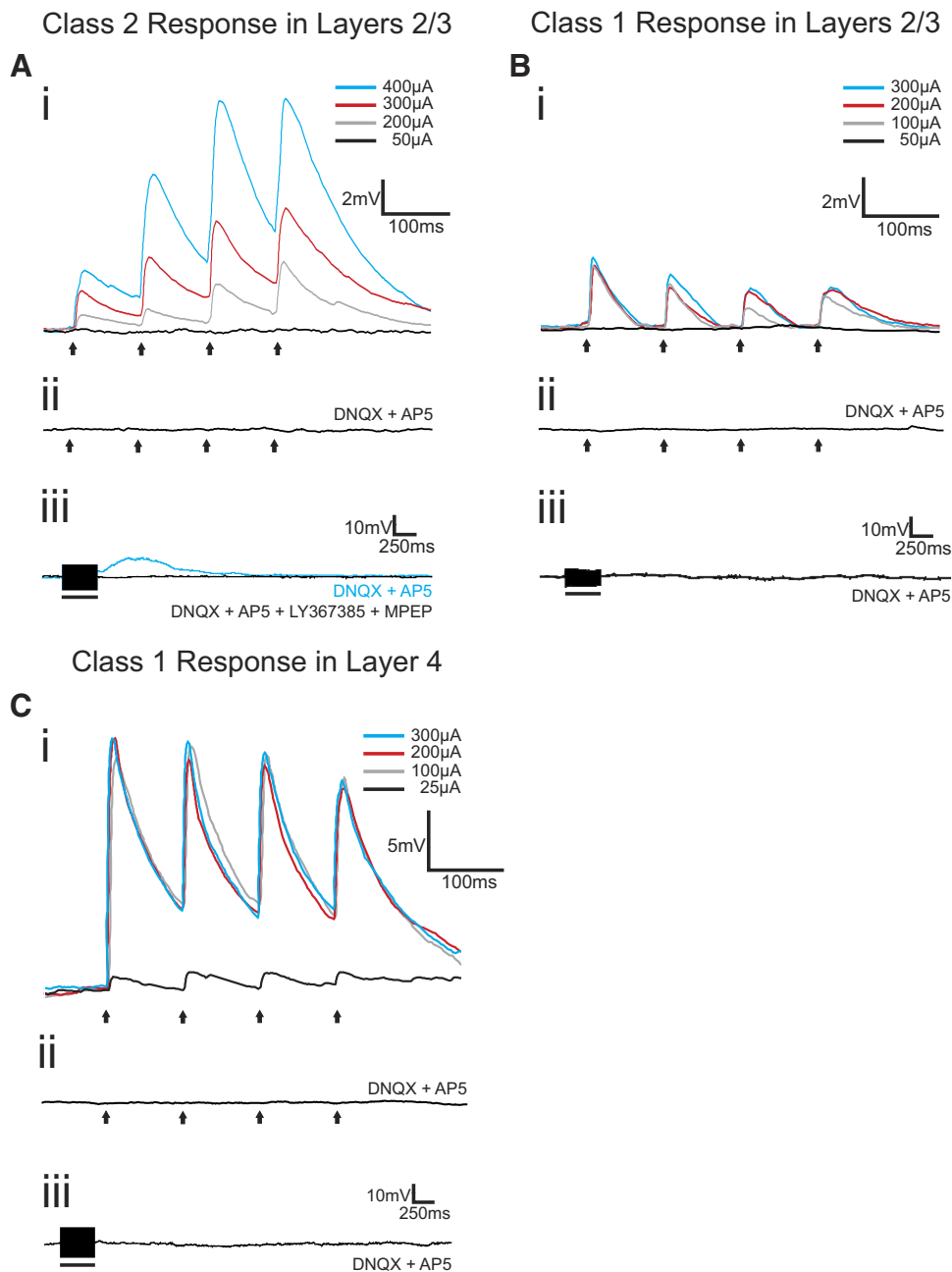


FIG. 3. Examples of Class 2 and Class 1 responses from cells in layers 2/3 and layer 4 of S1. **A:** Class 2 response in layers 2/3. **Ai:** the cell responded with paired-pulse facilitation to VPM stimulation at 10 Hz. Increasing stimulation intensities produced increases in excitatory postsynaptic potential (EPSP) amplitudes. **Aii:** stimulation at 10 Hz (250  $\mu$ A), in the presence of ionotropic glutamate receptor antagonists (DNQX and AP5), failed to produce any EPSPs. **Aiii:** high-frequency stimulation (HFS; 125 Hz, 250  $\mu$ A) in the presence of DNQX and AP5 produced a slow and prolonged membrane depolarization (blue trace) that could be blocked with a cocktail of type 1 (LY367385) and type 5 (MPEP) metabotropic glutamate receptor antagonists (black trace). **B:** Class 1 response in layers 2/3. **Bi:** this cell responded with paired-pulse depression to VPM stimulation at 10 Hz. EPSP amplitude was unaffected by increases in stimulation intensities. **Bii:** stimulation at 10 Hz (250  $\mu$ A), in the presence of DNQX and AP5, failed to produce any EPSPs. **Biii:** HFS (125 Hz, 250  $\mu$ A) in the presence of DNQX and AP5 did not produce any membrane potential changes. **C:** Class 1 response in layer 4. **Ci:** this cell responded with paired-pulse depression to VPM stimulation at 10 Hz. EPSP amplitude was unaffected by increases in stimulation intensities after a threshold was reached. **Cii:** stimulation at 10 Hz (250  $\mu$ A), in the presence of DNQX and AP5, failed to produce any EPSPs. **Ciii:** HFS (125 Hz, 250  $\mu$ A) in the presence of DNQX and AP5 did not produce any membrane potential changes. Arrows represent timing of stimulation for all 10 Hz trials, and black bars represent the duration of stimulation in HFS trials. Excluding HFS trials, all traces represent the average of 10 sweeps. Scale bars in **Ai**, **Bi**, and **Ci** apply to **Aii**, **Bii**, and **Cii**, respectively.

metabotropic glutamate receptor agonist 3,5-dihydroxyphenylglycine (DHPG, 250  $\mu$ M (Gereau and Conn 1995; Ito et al. 1992; Schoepp et al. 1994) while using a high  $Mg^{2+}$ /low  $Ca^{2+}$  ACSF (in mM: 0  $CaCl_2$ , 4  $MgCl_2$ ), which blocks synaptic transmission. We found that under these conditions, all cells responded to DHPG application with membrane depolarization (Supplemental Fig. S1A),<sup>1</sup> indicating the presence of group I metabotropic glutamate receptors located postsynaptically on the recorded cell. While this falls short of absolute proof that the metabotropic glutamate receptors activated from thalamocortical inputs are postsynaptic, this does seem to be the most parsimonious explanation of our data.

Class 1 responses were seen in a minority of cells in layers 2/3 (7 of 50 in S1 and 2 of 20 in A1). These cells responded with paired-pulse depression meaning that the amplitude of the second evoked EPSP in the series was less than that of the first (Figs. 3*Bi* and 4*Bi*). The Class 1 response was evoked in an all-or-none manner, meaning that the evoked EPSP amplitude rose abruptly to maximum value over a narrow range of stimulus intensities (Figs. 3*Bi* and 4*Bi*). As with the Class 2 response, ionotropic glutamate receptor antagonists blocked EPSPs evoked at 10 Hz (Figs. 3*Bii* and 4*Bii*), but unlike the Class 2 response, HFS did not then evoke any further response (Figs. 3*Biii* and 4*Biii*), reflecting the lack of metabotropic glutamate receptor activation over this pathway for Class 1 responses.

A third type of response observed in layers 2/3 cells of both S1 and A1 was one that combined characteristics of

<sup>1</sup> The online version of this article contains supplemental data.

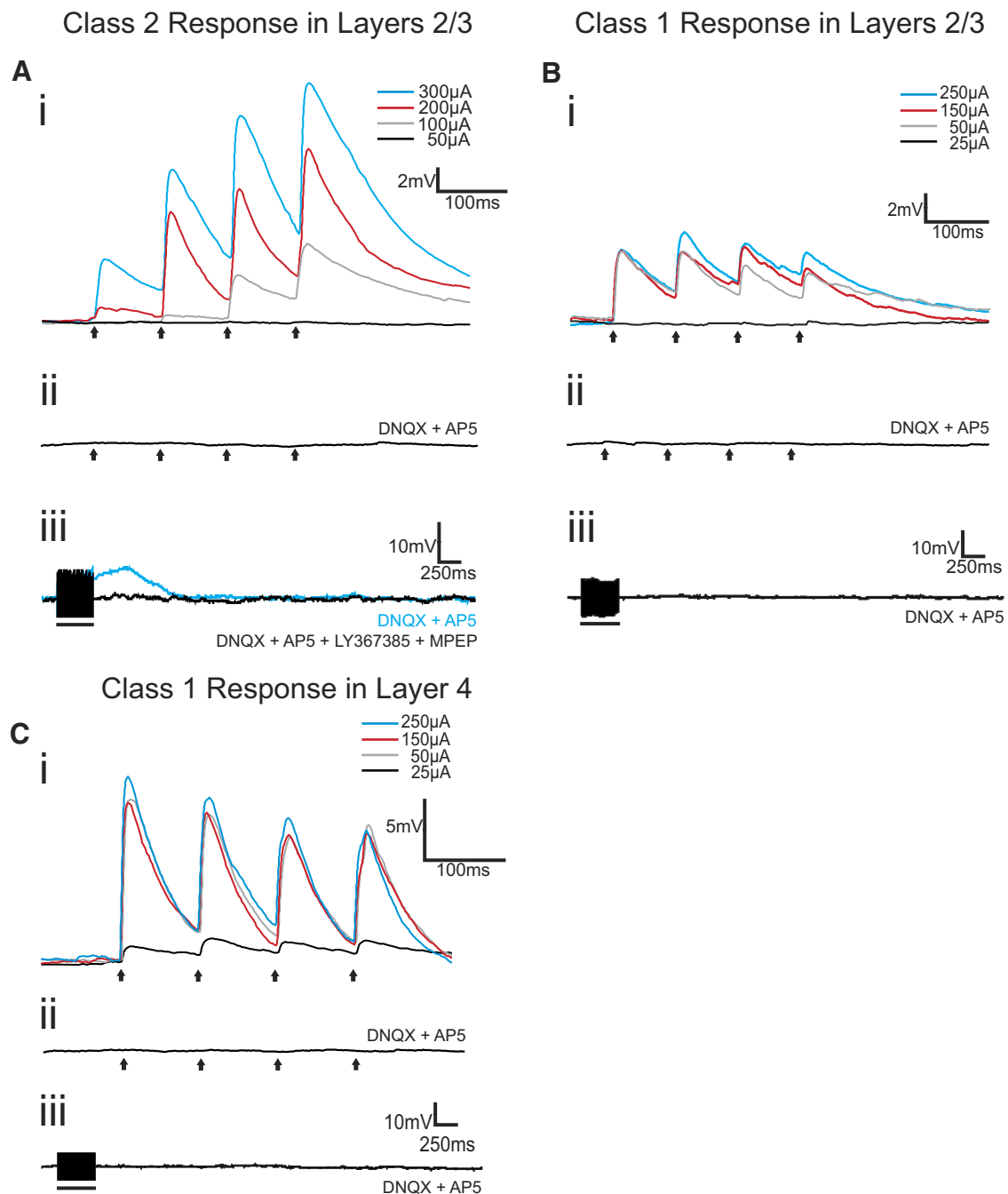


FIG. 4. Examples of Class 2 and Class 1 responses from cells in layers 2/3 and layer 4 of A1. **A**: Class 2 response in layers 2/3. **Ai**: the cell responded with paired-pulse facilitation to MGBv stimulation at 10 Hz. Increasing stimulation intensities produced increases in EPSP amplitudes. **Aii**: stimulation at 10 Hz (250  $\mu$ A), in the presence of ionotropic glutamate receptor antagonists (DNQX and AP5), failed to produce any EPSPs. **Aiii**: HFS (125 Hz, 200  $\mu$ A) in the presence of DNQX and AP5 produced a slow and prolonged membrane depolarization (blue trace) that could be blocked with a cocktail of type 1 (LY367385) and type 5 (MPEP) metabotropic glutamate receptor antagonists (black trace). **B**: Class 1 response in layers 2/3. **Bi**: this cell responded with paired-pulse depression to MGBv stimulation at 10 Hz. EPSP amplitude was unaffected by increases in stimulation intensities. **Bii**: stimulation at 10 Hz (250  $\mu$ A), in the presence of DNQX and AP5, failed to produce any EPSPs. **Biii**: HFS (125 Hz, 250  $\mu$ A) in the presence of DNQX and AP5 did not produce any membrane potential changes. **C**: Class 1 response in layer 4. **Ci**: this cell responded with paired-pulse depression to MGBv stimulation at 10 Hz. EPSP amplitude was unaffected by increases in stimulation intensities after a threshold was reached. **Cii**: stimulation at 10 Hz (250  $\mu$ A), in the presence of DNQX and AP5, failed to produce any EPSPs. **Ciii**: HFS (125 Hz, 200  $\mu$ A) in the presence of DNQX and AP5 did not produce any membrane potential changes. Arrows represent timing of stimulation for all 10 Hz trials, and black bars represent the duration of stimulation in HFS trials. Excluding HFS trials, all traces represent the average of 10 sweeps. Scale bars in **Ai**, **Bi**, and **Ci** apply to **Aii**, **Bii**, and **Cii**, respectively.

both classes described above, and therefore we refer to these thalamocortical responses as *Mixed*. More specifically, 11 cells (7 of 50 in S1 and 4 of 20 in A1) responded with

paired-pulse depression at minimal stimulation intensities that switched gradually to paired-pulse facilitation with increasing stimulus intensity (Fig. 5, **A** and **C**). Figure 5D

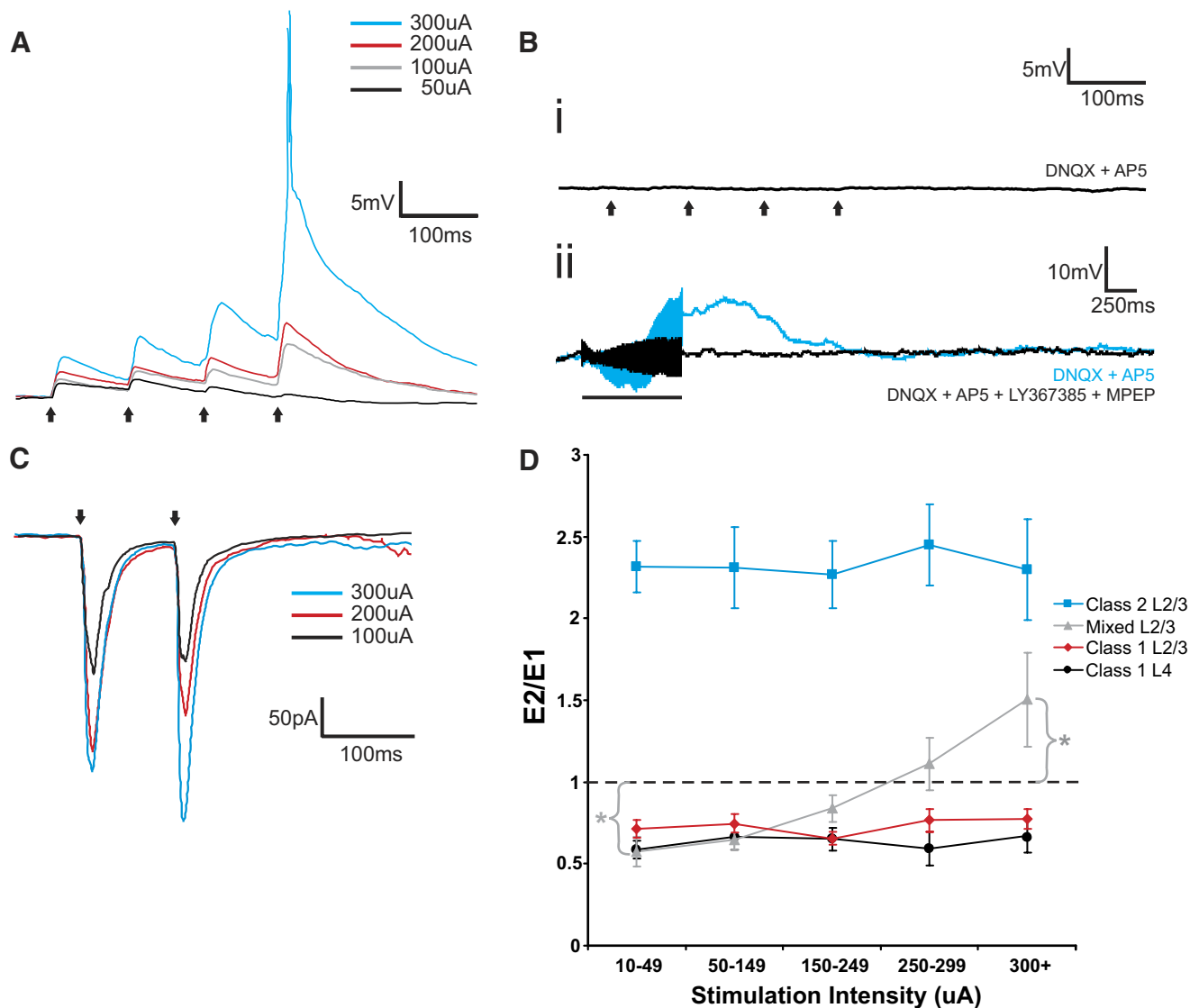


FIG. 5. Examples of Mixed responses from cells in layers 2/3 of S1 and A1. *A*: the short-term plasticity profile of a Mixed response recorded from S1 changed depending on the intensity of stimulation in VPM. At lower stimulation intensities, the cell responded with paired-pulse depression, whereas at higher stimulation intensities, it responded with paired-pulse facilitation. Increasing stimulation intensities produced increases in EPSP amplitudes. *Bi*: stimulation at 10 Hz (250  $\mu$ A) in the presence of ionotropic receptor antagonists (DNQX and AP5) failed to produce any EPSPs. *Bii*: HFS (125 Hz, 200  $\mu$ A) in the presence of DNQX and AP5 produced a slow and prolonged membrane depolarization (blue trace) that could be blocked with a cocktail of type 1 (LY367385) and type 5 (MPEP) metabotropic glutamate receptor antagonists (black trace). *C*: voltage-clamp recordings in a cell of A1 while stimulating MGBv at 10 Hz. At lower stimulation intensities, the cell responded with paired-pulse depression, whereas at higher stimulation intensities, it responded with paired-pulse facilitation. Increasing stimulation intensities produced increases in excitatory postsynaptic current (EPSC) amplitudes. Arrows represent timing of stimulation for all 10 Hz trials, and the black bar represents the duration of stimulation in the HFS trial. Excluding the HFS trial, all traces represent the average of 10 sweeps. *D*: changes in the E2/E1 ratio across stimulation intensities. Lines represent averages within each type of cells from both S1 and A1 (Error bars are SE). Whereas the E2/E1 ratios of cells exhibiting pure Class 1 and 2 responses remained either above or below 1 across stimulation intensities, for cells exhibiting Mixed responses, there was a transition from below 1 to above 1 as stimulation intensity increased. Wilcoxon's 1-sample rank sum tests: \* $P < 0.05$ .

shows this feature for the population of cells in this study, and whereas the cells showing pure Class 1 or 2 response properties exhibited a flat relationship between paired-pulse effects and stimulus intensity, there was a statistically significant shift in the cells exhibiting Mixed responses: Wilcoxon's one-sample rank sum tests confirmed that for the minimal stimulus intensity bin "10-49," the paired pulse ratio was  $<1$  ( $P < 0.05$ ), whereas for the highest stimulus intensity bin "300+," this ratio was  $>1$  ( $P < 0.05$ ). Finally, HFS in the presence of ionotropic glutamate receptor antagonists resulted in activation of group I metabotropic glutamate receptors (Fig. 5*Bii*). As described above for cells

exhibiting Class 2 responses, we performed an additional experiment on two cells exhibiting Mixed responses to determine whether the metabotropic glutamate receptor activation could be postsynaptic: these cells responded to DHPG application in the presence of high  $Mg^{2+}$ /low  $Ca^{2+}$  ACSF with membrane depolarization (Supplemental Fig. S1*B*).

**LAYER 4.** For comparison, we also recorded from layer 4 cells in both S1 and A1 while stimulating in VPM and MGBv, respectively, because previous work indicated that all layer 4 cells in these areas respond to thalamocortical input with what

we now call a Class 1 response profile but which was then referred to as a driver response (Lee and Sherman 2008). We thus recorded from 13 layer 4 cells in S1 (uncorrected membrane potential of  $-59.76 \pm 17.49$  mV and input resistance of  $555.25 \pm 171.68$  M $\Omega$ ) and 7 in A1 (uncorrected membrane  $-60.5 \pm 8.26$  mV and input resistance of  $520.36 \pm 131.49$  M $\Omega$ ). Every recorded layer 4 cell responded to thalamocortical stimulation with a Class 1 pattern (Figs. 3C and 4C), confirming the previous report (Lee and Sherman 2008).

Population data

Figure 6 shows various population data. Figure 6A indicates that, in both S1 and A1, most cells in layers 2/3 showed a Class

2 response. A minority of the cells in layers 2/3 responded with a Class 1 or Mixed profile. In comparing Class 1 and 2 responses in layers 2/3, Fig. 6B shows that the amplitudes of the first EPSP evoked at minimal stimulation intensities was considerably larger for Class 1 responses (Mann-Whitney: S1,  $P < 0.001$ ; A1,  $P < 0.001$ ; Fig. 6B), despite no significant differences in input resistance among these cells (Mann-Whitney: S1,  $P = 0.73$ ; A1,  $P = 0.40$ ). As a general trend, EPSP amplitudes in S1 were larger than those in A1, but these differences were not statistically significant, except for layer 4 cells (Mann-Whitney:  $P < 0.05$ ).

All cells with Class 2 responses of both cortices showed a protracted region of monotonic increases in EPSP ampli-

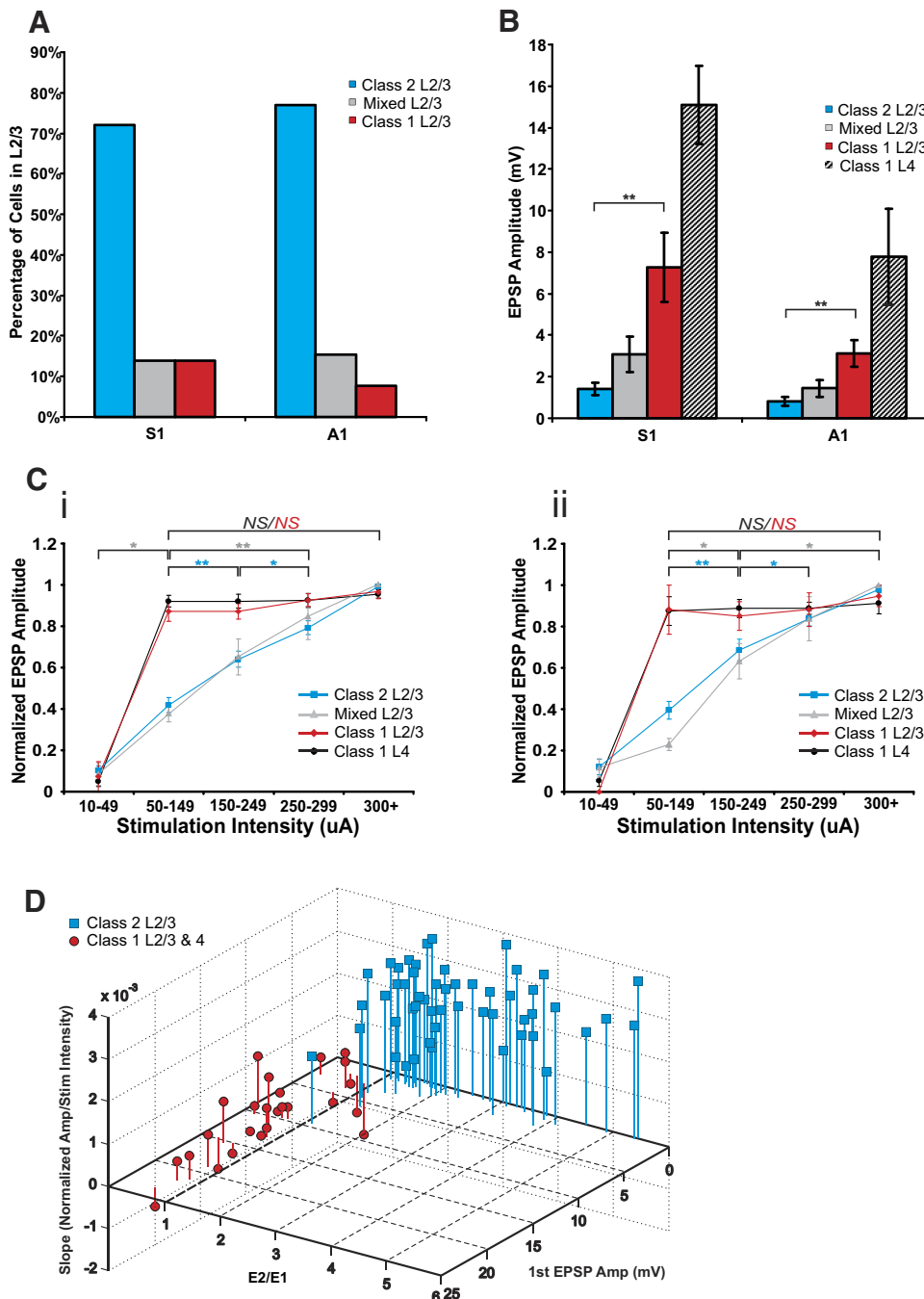


FIG. 6. Summary of response properties. A: proportions of cells with Classes 1 and 2 and Mixed responses found in layers 2/3 of S1 and A1. B: average 1st EPSP amplitude at minimal stimulation intensity. C: normalized 1st EPSP amplitudes for all cells across stimulation intensity bins for S1 (Ci) and A1 (Cii). Increases in stimulation intensity did not produce increases in EPSP amplitude for cells exhibiting Class 1 responses in layers 2/3 and layer 4 of both cortices once a threshold was reached (typically around 50  $\mu$ A). On the other hand, gradual increases in stimulation intensity resulted in gradual increases in EPSP amplitudes in cells exhibiting Class 2 and Mixed responses in layers 2/3 of both cortices. D: 3D scatter plot of 1st EPSP amplitude, E2/E1 ratio at minimal stimulation intensity, and slope of the normalized amplitude across stimulation intensities (50–300  $\mu$ A) for all cells with Class 1 and Class 2 responses in both cortices. All error bars represent SE. Mann-Whitney tests: \* $P < 0.05$ , \*\* $P < 0.001$ ; NS, not significant.

tude as stimulation intensity increased (see blue lines in Fig. 6, *Ci* and *Cii*). A Kruskal-Wallis test (S1,  $P < 0.001$ ; A1,  $P < 0.001$ ) and follow-up Mann-Whitney tests (Fig. 6) showed that EPSP amplitudes of high stimulation intensity bins were significantly larger than those of lower stimulation intensity bins, thus showing a graded effect. A similar graded relationship between stimulation intensity and EPSP amplitude was observed for cells of S1 and A1 with Mixed responses (see gray lines in Fig. 6, *Ci* and *Cii*; Kruskal-Wallis: S1,  $P < 0.001$ ; A1,  $P < 0.001$ ; see Fig. 6 for multiple contrasts). On the other hand, for cells with Class 1 responses in layers 2/3 of both cortices, once stimulation threshold was reached, further increases in stimulation intensity did not result in any increases in EPSP amplitude (see red lines in Fig. 6, *Ci* and *Cii*). A Kruskal-Wallis analysis on EPSP amplitudes across the highest four stimulation intensity bins confirmed that these values did not differ (S1,  $P = 0.26$ ; A1,  $P = 0.89$ ). This pattern was also observed in all layer 4 cells of S1 and A1 (see black lines in Fig. 6, *Ci* and *Cii*; Kruskal-Wallis: S1,  $P = 0.81$ ; A1,  $P = 0.96$ ).

To show that the parameters used to distinguish Class 1 from Class 2 responses were adequate, we created a three-dimensional scatter plot of the first EPSP amplitude, E2/E1 ratio, and slope of the normalized response amplitude across stimulation intensities (50–300  $\mu\text{A}$ ; Fig. 6D). We included data from layers 2/3 cells of both S1 and A1 exhibiting Class 2 responses and cells exhibiting Class 1 responses from layers 2/3 and 4 of both cortices. Cells with Mixed responses were excluded from this analysis because they were determined not to represent a separate class (see DISCUSSION). Class 2 responses were associated with small first EPSPs and larger slopes, and all cells exhibiting Class 2 responses had an E2/E1 ratio of  $>1$ . On the other hand, Class 1 responses always had E2/E1 ratios of  $<1$  and were associated with large first EPSPs and small slopes.

Given that age-related changes in layers 2/3 pyramidal neurons have been shown to occur over the 10–18 day age range (stabilizing near the end of this period; Oswald and Reyes 2008), we performed a series of analyses to study whether age impacted our measured responses. Regression analysis of first EPSP amplitude at minimal stimulation intensity versus age ( $R^2 = 0.02$ ,  $P = 0.3$ ), E2/E1 ratio versus age ( $R^2 = 0.001$ ,  $P = 0.84$ ), the slope of the normalized response amplitude across stimulation intensities (50–300  $\mu\text{A}$ ) versus age ( $R^2 = 0.0002$ ,  $P = 0.9$ ), and the maximum membrane potential change after high-frequency stimulation in the presence of ionotropic glutamate receptor antagonists versus age ( $R^2 = 0.02$ ,  $P = 0.23$ ) showed a lack of any significant age-related differences in parameters used to classify responses. Also, there was no significant difference in the ages of the animals in which we recorded Class 1 and 2 and Mixed responses (Kruskal-Wallis:  $P = 0.87$ ).<sup>2</sup>

The laminar position of recorded cells within layers 2/3 was measured for each class of cells in both cortices. In S1, recorded cells had an average distance of  $207 \pm 62 \mu\text{m}$  from the border of layers 3 and 4, whereas recorded cells in A1 had an average distance of  $78 \pm 21 \mu\text{m}$ . When comparing the laminar position of different classes of cells within each cortex,

no significant differences were found (Kruskal-Wallis: S1,  $P = 0.36$ ; A1,  $P = 0.40$ ). For purposes of comparison between S1 and A1 (layers 2/3 in S1 being much thicker than in A1), the laminar positions were calculated as a percentage of the distance from the layers 3–4 boundary to the pia (Fig. 7A).

An analysis of response latencies was performed for all classes of neurons. Layer 4 neurons in S1 responded to thalamic stimulation with a latency of  $3.39 \pm 1.88$  ms, whereas layers 2/3 neurons of S1 responded with a latency of  $4.96 \pm 2.34$  ms. Layer 4 neurons in A1 responded to thalamic stimulation with a latency of  $5.06 \pm 1.53$  ms, whereas layers 2/3 neurons of S1 responded with a latency of  $6.83 \pm 1.58$  ms. More specifically, with regard to layers 2/3 cells of S1, cells exhibiting Class 1 responses had a response latency of  $4.39 \pm 1.58$  ms, cells exhibiting Class 2 responses had a response latency of  $4.82 \pm 2.33$  ms, and cells exhibiting Mixed responses had a response latency of  $4.53 \pm 1.53$  ms; these response latencies were not significantly different from each other (Kruskal-Wallis:  $P = 0.86$ ). In layers 2/3 of A1, response latencies for cells exhibiting Class 1 responses were  $7.4 \pm 1.56$  ms, for cells with Class 2 responses,  $6.75 \pm 1.68$  ms, and for cells with Mixed responses,  $7.30 \pm 2.37$  ms. These response latencies were not significantly different (Kruskal-Wallis:  $P = 0.78$ ).

We performed regression analyses to assess the relationship between the laminar positions of recorded cells in layers 2/3 and their response latencies (Fig. 7A) and found significant correlations in both S1 ( $R^2 = 0.12$ ,  $P < 0.05$ ), and A1 ( $R^2 = 0.30$ ,  $P < 0.01$ ). Similarly, we performed regression analyses on first EPSP amplitude at minimal stimulation intensity versus response latency (Fig. 7B). These analyses showed no significant correlation in layers 2/3 neurons of S1 ( $R^2 = 0.049$ ,  $P = 0.12$ ) and A1 ( $R^2 = 0.001$ ,  $P = 0.87$ ).

#### Bouton sizes

BDA injections in VPM and MGBv produced extensive anterograde labeling in S1 and A1, respectively (Fig. 8, A and E). The average size of boutons in layer 4 (S1:  $1.21 \pm 0.52 \mu\text{m}^2$ ; A1:  $1.03 \pm 0.37 \mu\text{m}^2$ ) was significantly larger than those in layers 2/3 for both S1 ( $0.89 \pm 0.4 \mu\text{m}^2$ ) and A1 ( $0.47 \pm 0.19 \mu\text{m}^2$ ) (Fig. 8, B–D and F–H; Mann-Whitney: S1,  $P < 0.001$ ; A1,  $P < 0.001$ ). In addition, there was a significant difference in the size of boutons between layers 2/3 of S1 and A1 (Mann-Whitney:  $P < 0.001$ ), and between layers 4 of S1 and A1 (Mann-Whitney:  $P < 0.001$ ). As mentioned above, the EPSP amplitudes were also larger in S1 than in A1 (Fig. 6B), and this could not be attributed to differences in input resistance, because none were seen within groups of cells exhibiting the same response types (e.g., Class 1) or corresponding layers (e.g., layers 2/3) of S1 and A1 (Mann-Whitney: Class 1,  $P = 0.84$ ; Class 2,  $P = 0.37$ ; Mixed,  $P = 0.23$ ; layer 4,  $P = 0.68$ ; layers 2/3,  $P = 0.10$ ). At minimal stimulation intensities, first EPSP amplitudes were smaller in layers 2/3 than in layer 4 for both cortices (Fig. 6B). Because we observed larger EPSPs in areas with larger boutons (and smaller EPSPs in areas with smaller boutons), our data suggest a correlation between EPSP amplitude and bouton size (Li et al. 2003).

<sup>2</sup> It is worth noting that all three types of responses could be recorded from the same slice.

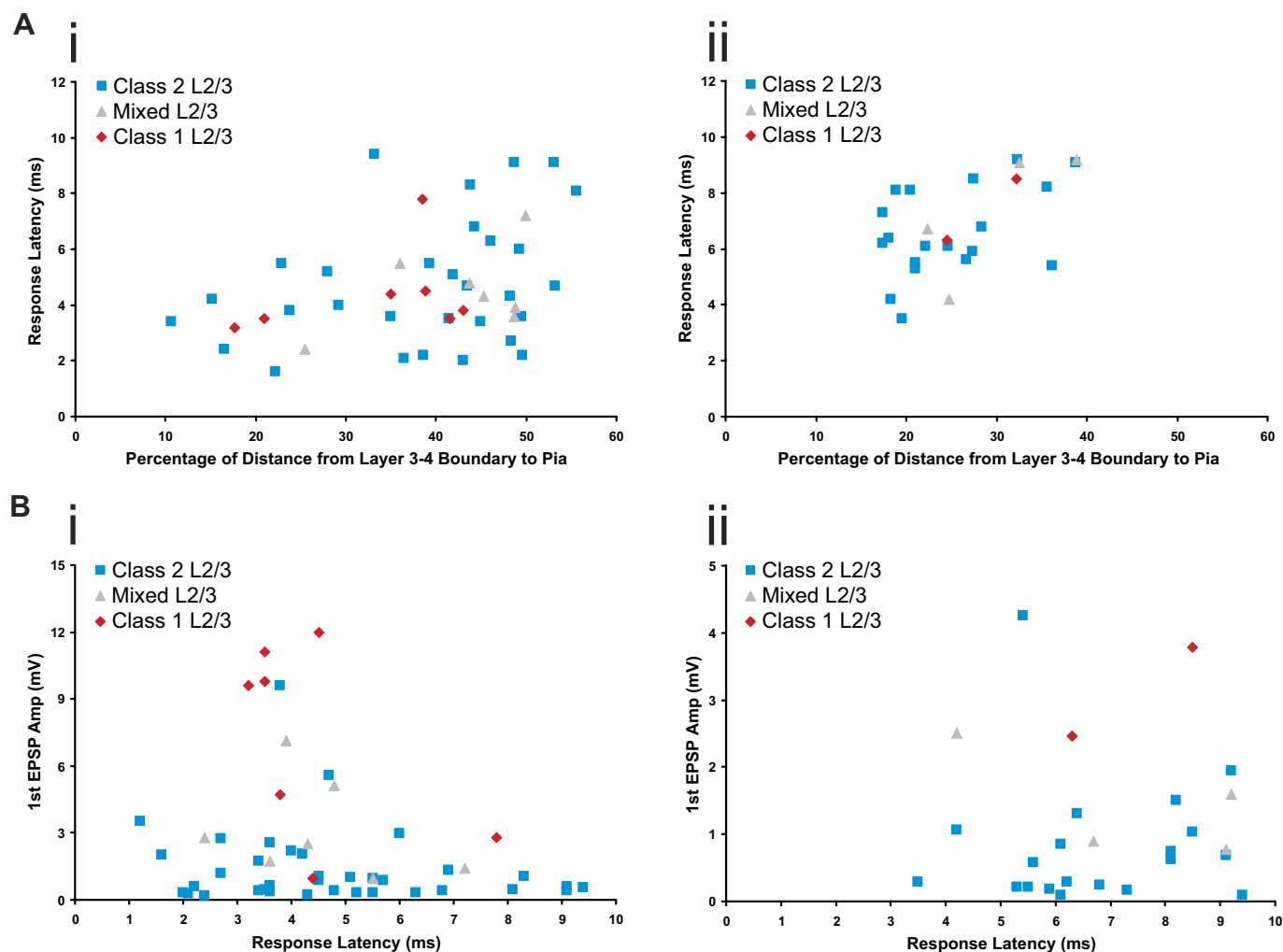


FIG. 7. Laminar positions and response latencies. *A*: scatter plots of the relationship between response latency and laminar position for layers 2/3 cells in S1 (*Ai*) and A1 (*Aii*). *B*: scatter plots of the relationship between 1st EPSP amplitude at minimal stimulation intensity and response latency for layers 2/3 neurons in S1 (*Bi*) and A1 (*Bii*).

## DISCUSSION

We found that stimulation of VPM and MGBv produced very similar responses in cells of S1 and A1, respectively, and that the overall responses seen in layers 2/3 differed from those seen in layer 4 for both cortices. Two distinct response patterns were observed, which we termed Class 1 and Class 2. The Class 1 response pattern includes larger initial EPSPs showing paired-pulse depression, an all-or-none activation profile, and only ionotropic glutamate receptor activation; the Class 2 response pattern includes smaller initial EPSPs showing paired-pulse facilitation, a graded activation profile, and both ionotropic and metabotropic glutamate receptor activation. All layer 4 cells responded to thalamic activation with Class 1 responses, as reported earlier (Lee and Sherman 2008). However, the large majority of responsive pyramidal neurons in layers 2/3 of S1 and A1 responded to thalamic stimulation with the Class 2 response pattern; the rest showed either a Class 1 response or what we interpreted as Mixed responses. Also, we found boutons of thalamocortical projections in layers 2/3 to be significantly smaller than those found in layer 4, suggesting that Class 2 responses may be associated with smaller boutons and Class 1 responses with larger boutons. These bouton size

measurements are consistent with previous anatomical data, which show a wide range of bouton sizes from small to large for afferents with Class 1 properties (Keller et al. 1985; Llano and Sherman 2008; Sur et al. 1987; Van Horn and Sherman 2004). Despite some overlap regarding some of their characteristics (e.g., 1st EPSP amplitude), Class 1 and Class 2 responses seem to be two distinct patterns of responses when one looks at all of their defining criteria in conjunction, including the presence or absence of any metabotropic glutamate receptor component, which is a qualitative parameter.

We observed a small number of cells in layers 2/3 of S1 and A1 that, on first appearance, seemed to exhibit responses that could not be identified as either Class 1 or 2 (we called these Mixed responses). One possibility is that these cells exhibited a third type of response that is neither Class 1 nor Class 2. We find a much more likely explanation to be that cells with Mixed responses receive convergent inputs that generate a mixture of Class 1 and 2 responses. At low stimulation intensities, Class 1 responses predominate because of their larger first EPSPs, and the cells respond to thalamic stimulation with paired-pulse depression. As stimulation intensity is increased, the Class 1 component of the Mixed cells' responses remains relatively

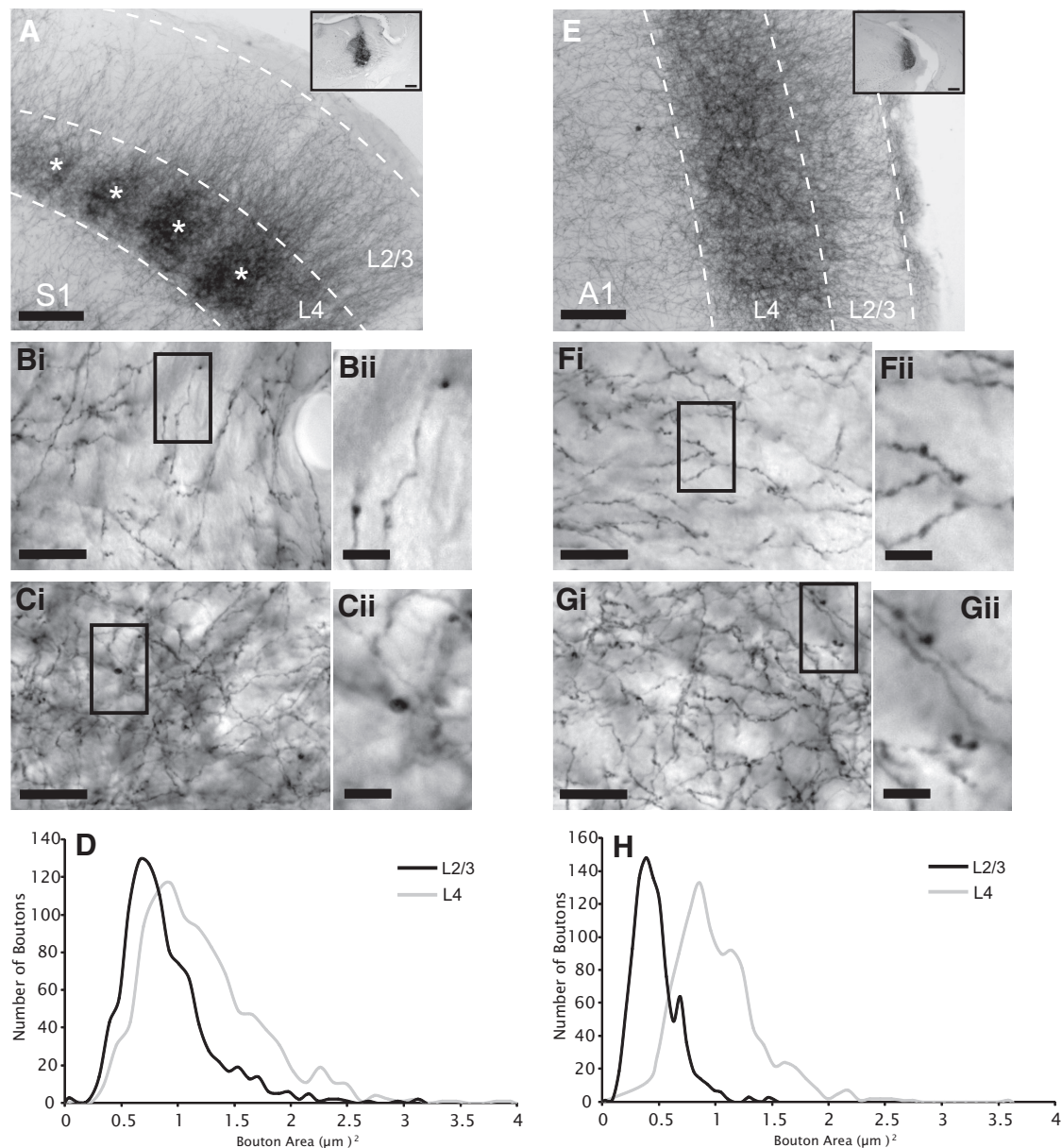


FIG. 8. Anterograde tracing of thalamic biotinylated dextran amine (BDA) injections. *A*: anterograde labeling of axons and boutons in barrel field of S1 after injection of BDA in VPM (*inset*). Asterisks represent individual barrels. *Bi*: BDA-labeled axons and boutons in layers 2/3 of S1. Highlighted area in *Bi* seen at higher magnification in *Bii*. *Ci*: BDA-labeled axons and boutons in layer 4 of S1. Highlighted area in *Ci* seen at higher magnification in *Cii*. *D*: histogram of bouton area in layers 2/3 and layer 4 of S1 ( $\mu\text{m}^2$ ). *E*: anterograde labeling of axons and boutons in A1 after injection of BDA in MGBv (*inset*). *Fi*: BDA-labeled axons and boutons in layers 2/3 of A1. Highlighted area in *Fi* seen at higher magnification in *Fii*. *Gi*: BDA-labeled axons and boutons in layer 4 of A1. Highlighted area in *Gi* seen at higher magnification in *Gii*. *H*: histogram of bouton area in layers 2/3 and layer 4 of A1 ( $\mu\text{m}^2$ ). Scale bars: *A* and *E insets*, 0.25 mm; *Bi*, *Ci*, *Fi*, and *Gi*, 20  $\mu\text{m}$ ; *Bii*, *Cii*, *Fii*, and *Gii*, 5  $\mu\text{m}$ .

constant, whereas the Class 2 component begins to play a larger role. The increasing contribution of the Class 2 component causes the EPSP amplitudes to increase as stimulation intensity increases, and eventually, the Class 2 properties come to dominate, thus causing the cells to respond to thalamic stimulation with paired-pulse facilitation. Assuming this hypothesis is correct, Mixed responses are not a third, unique, class of response pattern, but rather a mixture of Class 1 and Class 2 responses. It needs to be noted that the number of cells in layers 2/3 that showed Mixed responses may have been somewhat underestimated in our slice preparations, given that inputs of different synaptic properties that may have otherwise

converged on single cells could have been severed because of the slicing angles we used.

Previous work in S1 using the original somatosensory thalamocortical slice (Agmon and Connors 1991) reported that only ~8% of layer 2/3 neurons received monosynaptic input from thalamus (Bureau et al. 2006). Even though we only found connectivity in 40% of our recorded cells, this is still a higher percentage than previously described. We believe this is likely because of a few differences in our preparation. Our somatosensory slice was an adaptation of the original Agmon and Connors (1991) slice and has been shown to preserve connectivity to the upper layers of barrel cortex (Linas et al.

2002), making it ideal for our purposes. In addition, our slices were 150  $\mu\text{m}$  thicker than those used by Bureau et al. and were thus more likely to contain more intact thalamocortical fibers.

#### *Evidence for monosynaptic inputs*

The monosynaptic nature of the responses seen in layers 2/3 is supported by a number of factors. The EPSPs that we recorded were consistent in both their shape and time of onset across multiple trials for a single cell (criteria that have been used to distinguish monosynaptic input, Beierlein and Connors 2002). In addition, even though the latencies we observed in layers 2/3 were longer than those seen in layer 4 by roughly 1.5 ms in both cortices, it is unlikely that the responses recorded in layers 2/3 cells were disynaptic. In a study of synaptically coupled layer 4 spiny neurons and layers 2/3 pyramidal neurons in S1 (Feldmeyer et al. 2002), the latency between a spike in the layer 4 neuron and the onset of an EPSP in the layers 2/3 neuron was found to be just over 2 ms. Given that we measured latency as the time between stimulation and the initiation of an EPSP, the 1.5 ms discrepancy between our layers 4 and 2/3 cells is not long enough to account for the rise time and initiation of a spike in the layer 4 neuron and an additional 2 ms for synaptic transmission between the two layers. Also, the same study showed that the layer 4 input to layers 2/3 pyramidal neurons exhibits paired-pulse depression. As we observed mainly paired-pulse facilitation in our layers 2/3 cells (Class 2 responses), it is unlikely that their input was coming from layer 4. Moreover, the latencies of our Class 1 and Mixed responses (which exhibited paired-pulse depression at lower stimulation intensities) were not significantly different from those of Class 2 responses, and it is therefore unlikely that their inputs were disynaptic. Finally, in our layers 2/3 neurons, we observed a positive correlation between response latency and the distance of the recorded cell from the layers 3–4 boundary. This correlation is likely because of conduction time in thalamocortical axons; longer latencies being associated with action potentials having to travel further into layers 2/3.

Because of the time course of evoked metabotropic glutamate receptor responses, we could not use latency measures to determine whether these were activated monosynaptically or via intermediary cortical circuitry. Given that all ionotropic glutamate receptors were blocked during high-frequency stimulation trials, it is unlikely that thalamocortical axons would be able to drive other neurons that would then activate metabotropic glutamate receptors on the recorded cell. Also, and perhaps more importantly, what is of particular interest is that in cells exhibiting Class 2 and Mixed responses, we were able to activate mGluRs, whereas we were unable to do so in cells exhibiting Class 1 responses. What is central to our findings is either the presence or absence of a metabotropic glutamate receptor response after thalamic stimulation, but we conclude that the mGluR responses seen here were indeed monosynaptically evoked from thalamus.

#### *Relating thalamocortical projections to drivers and modulators*

We found all the synaptic properties and anatomical features associated with Class 1 and Class 2 responses in layers 2/3 and 4 of cortex to strongly resemble those of drivers and modula-

tors, respectively, seen in thalamus (Reichova and Sherman 2004; Sherman and Guillery 2006).<sup>3</sup> In sensory thalamic nuclei, drivers are known to be the main source of information to be relayed and thus determine the main receptive field properties of the postsynaptic relay cells, whereas modulators influence the way relay cells transmit this driver input to cortex (Sherman and Guillery 1998). Although in the thalamus, the terms driver and modulator imply functional significance, the same cannot be automatically assumed for thalamocortical projections, which is the main reason we have adopted the different terminology of Class 1 and 2.

Nonetheless, the features of Class 1 and 2 responses described here are consistent with the idea that, for these thalamocortical inputs, the former is well suited for the reliable transfer of information and the latter, for modulation. For instance, the main information input should elicit large EPSPs. Also, paired-pulse depression is usually associated with high probability of transmitter release (Dobrunz and Stevens 1997), and it may dynamically regulate neuronal sensitivity during rapid changes in sensory input (Chung et al. 2002). Finally, and perhaps most importantly, lack of a metabotropic glutamate receptor response for Class 1 inputs ensures relatively brief EPSPs, allowing a more faithful relay of temporal information (for the sake of simplicity, we will henceforth refer to inputs responsible for Class 1 and Class 2 responses as Class 1 and Class 2 inputs, respectively). Class 2 inputs, by being weaker and more convergent (as indicated by their graded activation profile), can combine in many different ways to provide a variety of modulatory functions. Also, the metabotropic glutamate receptor response not only provides a relatively prolonged modulation of excitability, but the sustained effects on membrane potential mean a more effective control over the several time- and voltage-dependent conductances that have relatively long time constants for inactivation kinetics (e.g.,  $I_T$ ,  $I_h$ , and  $I_A$ ; reviewed in Sherman and Guillery 1996, 2006). Furthermore, the metabotropic glutamate receptor activation outlasts activity of the input, often by seconds (Govindaiah and Cox 2004), further distorting temporal information. Given our findings and those of previous work (Lee and Sherman 2008), it is likely that cells exhibiting Class 1 responses are receiving driving input, cells exhibiting Class 2 responses are receiving modulatory input, and cells exhibiting Mixed responses receive convergent driving and modulatory inputs from thalamus.

#### *Origins of Class 1 and Class 2 inputs*

A question that needs to be addressed concerns the origins of these two different classes of input. In the visual system of both cats and primates, different classes of geniculocortical cells project to different layers. In the cat, X and Y cells project to layer 4, whereas W cells project to layers 2/3 (Anderson et al. 2009; Ferster and Levay 1978), and in the primate, parvocellular and magnocellular cells project to layer 4, whereas koniocellular cells project to layers 2/3 (Ding and Casagrande 1997; Shostak et al. 2003). Although analogous pathways have

<sup>3</sup> Note that parameters within a class may show considerable variability, and this variation may be greater than variation seen between classes. For example, variation within any trout species may be greater than that seen between hyenas and leopards. Thus, even though the individual parameters of these thalamocortical afferents may not coincide precisely with those of thalamic drivers or modulators, this would not rule out a common class.

not been described in the somatosensory or auditory systems, it is nonetheless possible that two separate populations of thalamic relay cells exist in these systems, one providing Class 1 input to layer 4 and the other Class 2 input to layers 2/3. If this holds true, an extension of this logic suggests another interesting hypothesis: in the visual system of cats (and monkeys), X and Y (parvocellular and magnocellular) cells provide a Class 1 or driver input to layer 4, whereas W (koniocellular) cells provide mostly a Class 2 or modulatory input to layers 2/3.

Another possibility is that a single relay neuron could be providing both Class 1 and Class 2 inputs to cortex in our experiments. If this were true, it raises a question regarding branching thalamic axons; that is, if a thalamic relay cell provides a certain type of input (e.g., Class 1) to one set of postsynaptic neurons, could it provide a different type of input (e.g., Class 2) to some of its other neuronal targets? Studies in cortex and hippocampus have shown that a single axon can elicit different postsynaptic response properties at different synaptic sites (Pelkey and McBain 2007, 2008; Reyes et al. 1998). Evidence exists that all thalamic relay neurons found in rodent VPM and the vast majority of relay neurons in MGBv do not project to layers 2/3 without also forming synapses in layer 4 (Arnold et al. 2000; Jones 1998, 2009; Oda et al. 2004; Rubio-Garrido et al. 2009). If correct, this implies that the thalamocortical neurons providing Class 2 inputs to layers 2/3 must also provide Class 1 inputs to layer 4. If Class 1 inputs are mainly information bearing and Class 2 are modulatory, a further implication of this is that a single thalamocortical neuron can modulate a cell in layers 2/3 while it drives a cell in layer 4.

#### *Inputs to layers 2/3 pyramidal neurons*

Aside from thalamic projections, pyramidal neurons in layers 2/3 also receive other glutamatergic inputs from layer 4 (among other sources). Evidence exists that these inputs show paired-pulse depression (Feldmeyer et al. 2002; Oswald and Reyes 2008), suggesting that they may be Class 1, or driver in nature. Current dogma asserts that information arrives in layer 4 of cortex via the thalamus and is transmitted from layer 4 to layers 2/3 (Gilbert and Wiesel 1979). This fits the notion that these two pathways (thalamocortical to layer 4 and layer 4 to layers 2/3) are Class 1 or drivers. In this context, our evidence suggests that most thalamocortical inputs to layers 2/3 modulate the circuit from layer 4 to layers 2/3, although exactly how remains unknown.

#### *Thalamus as a modulator of cortex*

Because all previously studied thalamic projections were classified as Class 1 (drivers) (Lee and Sherman 2008), this is the first demonstration of Class 2 (modulatory) projections originating in thalamus. Because the majority of cells in layers 2/3 exhibited pure Class 2 responses, thalamic input to layers 2/3 seems to be predominantly modulatory. Furthermore, if our conclusion is correct that cells exhibiting what we term Mixed responses indeed receive converging driving and modulatory inputs and not a unique, third type of input, we only observed two types of glutamatergic inputs to layers 2/3 from thalamus, and these types (Class 1 or driver and Class 2 or modulator) are the same as described for other thalamic and cortical pathways (Lee and

Sherman 2008–2010; Petrof and Sherman 2009; Reichova and Sherman 2004). It thus follows that our data provide further evidence that thalamus is more than just a simple relay of sensory information and suggest that thalamus continues to directly modulate ascending sensory information even after it reaches cortex.

#### GRANTS

This work was supported by National Institute on Deafness and Other Communication Disorders Grant DC008794 to S. M. Sherman and National Institute of General Medical Sciences Medical Scientist National Research Service Award 5 T32 GM07281 to A. N. Viaene.

#### DISCLOSURES

No conflicts of interest, financial or otherwise, are declared by the authors.

#### REFERENCES

- Agmon A, Connors BW.** Thalamocortical responses of mouse somatosensory (barrel) cortex in vitro. *Neuroscience* 41: 365–379, 1991.
- Anderson JC, da Costa NM, Martin KA.** The W cell pathway to cat primary visual cortex. *J Comp Neurol* 516: 20–35, 2009.
- Arnold PB, Li CX, Waters RS.** Thalamocortical arbors extend beyond single cortical barrels: an in vivo intracellular tracing study in rat. *Exp Brain Res* 136: 152–168, 2000.
- Beierlein M, Connors BW.** Short-term dynamics of thalamocortical and intracortical synapses onto layer 6 neurons in neocortex. *J Neurophysiol* 88: 1924–1932, 2002.
- Bureau I, von Saint Paul F, Svoboda K.** Interdigitated paralemniscal and lemniscal pathways in the mouse barrel cortex. *PLoS Biol* 4: e382, 2006.
- Chung S, Li X, Nelson SB.** Short-term depression at thalamocortical synapses contributes to rapid adaptation of cortical sensory responses in vivo. *Neuron* 34: 437–446, 2002.
- Cruikshank SJ, Rose HJ, Metherate R.** Auditory thalamocortical synaptic transmission in vitro. *J Neurophysiol* 87: 361–384, 2002.
- Ding Y, Casagrande VA.** The distribution and morphology of LGN K pathway axons within the layers and CO blobs of owl monkey V1. *Vis Neurosci* 14: 691–704, 1997.
- Dobrunz LE, Stevens CF.** Heterogeneity of release probability, facilitation, and depletion at central synapses. *Neuron* 18: 995–1008, 1997.
- Dudek SM, Friedlander MJ.** Intracellular blockade of inhibitory synaptic responses in visual cortical layer IV neurons. *J Neurophysiol* 75: 2167–2173, 1996.
- Feldmeyer D, Lübke J, Silver RA, Sakmann B.** Synaptic connections between layer 4 spiny neurone-layer 2/3 pyramidal cell pairs in juvenile rat barrel cortex: physiology and anatomy of interlaminar signalling within a cortical column. *J Physiol* 538: 803–822, 2002.
- Ferster D, LeVay S.** The axonal arborizations of lateral geniculate neurons in the striate cortex of the cat. *J Comp Neurol* 182: 923–944, 1978.
- Franklin KBJ, Paxinos G.** *The Mouse Brain in Stereotaxic Coordinates*. San Diego, CA: Academic Press, 2008.
- Friedlander MJ, Lin CS, Stanford LR, Sherman SM.** Morphology of functionally identified neurons in lateral geniculate nucleus of the cat. *J Neurophysiol* 46: 80–129, 1981.
- Gereau RW IV, Conn PJ.** Roles of specific metabotropic glutamate receptor subtypes in regulation of hippocampal CA1 pyramidal cell excitability. *J Neurophysiol* 74: 122–129, 1995.
- Gilbert CD, Wiesel TN.** Morphology and intracortical projections of functionally characterised neurones in the cat visual cortex. *Nature* 280: 120–125, 1979.
- Govindaiah, Cox CL.** Synaptic activation of metabotropic glutamate receptors regulates dendritic outputs of thalamic interneurons. *Neuron* 41: 611–623, 2004.
- Ito I, Kohda A, Tanabe S, Hirose E, Hayashi M, Mitsunaga S, Sugiyama H.** 3,5-Dihydroxyphenyl-glycine: a potent agonist of metabotropic glutamate receptors. *Neuroreport* 3: 1013–1016, 1992.
- Jones EG.** A new view of specific and nonspecific thalamocortical connections. *Adv Neurol* 77: 49–73, 1998.
- Jones EG.** Thalamic circuitry and thalamocortical synchrony. *Philos Trans R Soc Lond B Biol Sci* 357: 1659–1673, 2009.

- Keller A, White EL, Cipolloni PB.** The identification of thalamocortical axon terminals in barrels of mouse Sml cortex using immunohistochemistry of anterogradely transported lection (*Phaseolus vulgaris*-leucoagglutinin). *Brain Res* 343: 159–165, 1985.
- Lam YW, Nelson CS, Sherman SM.** Mapping of the functional interconnections between thalamic reticular neurons using photostimulation. *J Neurophysiol* 96: 2593–2600, 2006.
- Lam YW, Sherman SM.** Mapping by laser photostimulation of connections between the thalamic reticular and ventral posterior lateral nuclei in the rat. *J Neurophysiol* 94: 2472–2483, 2005.
- Lam YW, Sherman SM.** Different topography of the reticulothalamic inputs to first- and higher-order somatosensory thalamic relays revealed using photostimulation. *J Neurophysiol* 98: 2903–2909, 2007.
- Lee CC, Sherman SM.** Synaptic properties of thalamic and intracortical inputs to layer 4 of the first- and higher-order cortical areas in the auditory and somatosensory systems. *J Neurophysiol* 100: 317–326, 2008.
- Lee CC, Sherman SM.** Modulator property of the intrinsic cortical projection from layer 6 to layer 4. *Front Syst Neurosci* 3: 3, 2009.
- Lee CC, Sherman SM.** Topography and physiology of ascending streams in the auditory tectothalamic pathway. *Proc Natl Acad Sci USA* 107: 372–377, 2010.
- Li J, Guido W, Bickford ME.** Two distinct types of corticothalamic EPSPs and their contribution to short-term synaptic plasticity. *J Neurophysiol* 90: 3429–3440, 2003.
- Llano DA, Sherman SM.** Evidence for nonreciprocal organization of the mouse auditory thalamocortical-corticothalamic projection systems. *J Comp Neurol* 507: 1209–1227, 2008.
- Llano DA, Theyel BB, Mallik AK, Sherman SM, Issa NP.** Rapid and sensitive mapping of long-range connections in vitro using flavoprotein autofluorescence imaging combined with laser photostimulation. *J Neurophysiol* 101: 3325–3340, 2009.
- Llinas RR, Leznik E, Urbano FJ.** Temporal binding via cortical coincidence detection of specific and nonspecific thalamocortical inputs: a voltage-dependent dye-imaging study in mouse brain slices. *Proc Natl Acad Sci USA* 99: 449–454, 2002.
- McCormick DA, von Krosigk M.** Corticothalamic activation modulates thalamic firing through glutamate “metabotropic” receptors. *Proc Natl Acad Sci USA* 89: 2774–2778, 1992.
- Oda S, Kishi K, Yang J, Chen S, Yokofujita J, Igarashi H, Tanihata S, Kuroda M.** Thalamocortical projection from the ventral posteromedial nucleus sends its collaterals to layer I of the primary somatosensory cortex in rat. *Neurosci Lett* 367: 394–398, 2004.
- Oswald AM, Reyes AD.** Maturation of intrinsic and synaptic properties of layer 2/3 pyramidal neurons in mouse auditory cortex. *J Neurophysiol* 99: 2998–3008, 2008.
- Pelkey KA, McBain CJ.** Differential regulation at functionally divergent release sites along a common axon. *Curr Opin Neurobiol* 17: 366–373, 2007.
- Pelkey KA, McBain CJ.** Target-cell-dependent plasticity within the mossy fibre-CA3 circuit reveals compartmentalized regulation of presynaptic function at divergent release sites. *J Physiol* 586: 1495–502, 2008.
- Petrof I, Sherman SM.** Synaptic properties of the mammillary and cortical afferents to the anterodorsal thalamic nucleus in the mouse. *J Neurosci* 29: 7815–7819, 2009.
- Reichova I, Sherman SM.** Somatosensory corticothalamic projections: distinguishing drivers from modulators. *J Neurophysiol* 92: 2185–2197, 2004.
- Reyes A, Lujan R, Rozov A, Burnashev N, Somogyi P, Sakmann B.** Target-cell-specific facilitation and depression in neocortical circuits. *Nat Neurosci* 1: 279–285, 1998.
- Rubio-Garrido P, Pérez-de-Manzo F, Porrero C, Galazo MJ, Clascá F.** Thalamic input to distal apical dendrites in neocortical layer I is massive and highly convergent. *Cereb Cortex* 19: 2380–2395, 2009.
- Schoepp DD, Goldsworthy J, Johnson BG, Salhoff CR, Baker SR.** 3,5-dihydroxyphenylglycine is a highly selective agonist for phosphoinositide-linked metabotropic glutamate receptors in the rat hippocampus. *J Neurochem* 63: 769–772, 1994.
- Shepherd GM, Pologruto TA, Svoboda K.** Circuit analysis of experience-dependent plasticity in the developing rat barrel cortex. *Neuron* 38: 277–289, 2003.
- Sherman SM, Guillery RW.** Functional organization of thalamocortical relays. *J Neurophysiol* 76: 1367–1395, 1996.
- Sherman SM, Guillery RW.** On the actions that one nerve cell can have on another: distinguishing “drivers” from “modulators”. *Proc Natl Acad Sci USA* 95: 7121–7126, 1998.
- Sherman SM, Guillery RW.** *Exploring the Thalamus*. Cambridge, MA: MIT Press, 2006.
- Shibuki K, Hishida R, Murakami H, Kudoh M, Kawaguchi T, Watanabe M, Watanabe S, Kouuchi T, Tanaka R.** Dynamic imaging of somatosensory cortical activity in the rat visualized by flavoprotein autofluorescence. *J Physiol* 549: 919–927, 2003.
- Shostak Y, Ding Y, Casagrande VA.** Neurochemical comparison of synaptic arrangements of parvocellular, magnocellular, and koniocellular geniculate pathways in owl monkey (*Aotus trivirgatus*) visual cortex. *J Comp Neurol* 456: 12–28, 2003.
- Slyter E.** *Optical Methods in Biology*. New York: Wiley-Interscience, 1970.
- Sur M, Esguerra M, Garraghty PE, Kritzer MF, Sherman SM.** Morphology of physiologically identified retinogeniculate X- and Y-axons in the cat. *J Neurophysiol* 58: 1–32, 1987.
- Tan Z, Hu H, Huang ZJ, Agmon A.** Robust but delayed thalamocortical activation of dendritic-targeting inhibitory interneurons. *Proc Natl Acad Sci USA* 105: 2187–2192, 2008.
- Van Horn SC, Sherman SM.** Differences in projection patterns between large and small corticothalamic terminals. *J Comp Neurol* 475: 406–415, 2004.
- Zhou Y, Liu BH, Wu GK, Kim YJ, Xiao Z, Tao HW, Zhang LI.** Preceding inhibition silences layer 6 neurons in auditory cortex. *Neuron* 65: 706–717, 2010.